

Anomalous Transverse Relaxation in ^1H Spectroscopy in Human Brain at 4 Tesla

Stefan Posse, Charles Andre Cuenod, Robert Risinger, Denis Le Bihan, Robert S. Balaban

Longitudinal (T_1) and apparent transverse relaxation times (T_2) of choline-containing compounds (Cho), creatine/phosphocreatine (Cr/PCr), and *N*-acetyl aspartate (NAA) were measured *in vivo* in human brain at 4 Tesla. Measurements were performed using a water suppressed stimulated echo pulse sequence with complete outside volume presaturation to improve volume localization at short echo times. T_1 -values of Cho (1.2 ± 0.1 s), Cr (1.6 ± 0.3 s), and NAA (1.6 ± 0.2 s) at 4 Tesla in occipital brain were only slightly larger than those reported in the literature at 1.5 Tesla. Thus, TR will not adversely affect the expected enhancement of signal-to-noise at 4 Tesla. Surprisingly, apparent T_2 -values of Cho (142 ± 34 ms), Cr (140 ± 13 ms), and NAA (185 ± 24 ms) at 4 Tesla were significantly smaller than those at 1.5 Tesla and further decreased when increasing the mixing interval TM . Potential contributing factors, such as diffusion in local susceptibility related gradients, dipolar relaxation due to intracellular paramagnetic substances and motion effects are discussed. The results suggest that short echo time spectroscopy is advantageous to maintain signal to noise at 4 Tesla.

Key words: nuclear magnetic resonance spectroscopy; relaxation; diffusion; proton spectroscopy.

INTRODUCTION

Longitudinal (T_1) and transverse (T_2) relaxation times are key parameters in localized proton (^1H) spectroscopy, because they determine spectral sensitivity and play an important role in understanding molecular organization *in vivo*. They directly effect the design of spectroscopy pulse sequences and the selection of pulse sequence parameters. Differences among ^1H -relaxation times of different metabolite resonances, water and mobile fatty acids can be used to enhance spectral localization and to extract spectral information of interest. For example, brain spectroscopy at clinical field strengths is frequently performed at long echo times to facilitate localization by attenuating overwhelming resonances from water and

extracranial fat which exhibit much shorter T_2 -relaxation times than the dominant singlet resonances from choline (CHO), creatine (CR), and *N*-acetyl-aspartate (NAA). Metabolite resonances with short T_2 -relaxation times and J -coupling are attenuated as well at long echo times which facilitates spectral interpretation. However, preliminary experiments in human and animal brain suggest that T_2 -values of metabolite signals are species dependent (1–6) and may change with disease (7–9). This will confound spectral quantitation at long echo times unless T_2 -values are precisely measured.

Recently, increased magnetic field strengths of up to 4 Tesla became available for human studies. Preliminary reports indicate that considerable gains in spectral resolution and sensitivity as compared with clinical field strengths can be achieved (10–15). However, T_1 -values are expected to increase with field strengths thus reducing the signal-to-noise advantage gained by the higher field strength (16). From theoretical considerations T_2 -values are expected to be independent of field strength (16). However, preliminary results from our laboratory (17), which have been confirmed by Hetherington and coworkers (13) indicate that the apparent T_2 -values of metabolite resonances in human brain decrease with increasing field strength. In this paper we present a more complete account of our measurements of metabolite T_1 -values and apparent T_2 -values in normal human brain at 1.5 and 4 Tesla.

MATERIALS AND METHODS

Relaxation measurements on normal volunteers ($n = 16$) were performed on an experimental 4 Tesla whole body scanner (General Electric Medical Systems, Milwaukee, WI). One study was performed at a clinical 1.5 Tesla whole body scanner (General Electric Medical Systems, Milwaukee, WI) to confirm methodology and literature values at that field strength. Both scanners were equipped with 10 mT/m actively shielded gradient coils. Informed consent was obtained from all volunteers prior to the measurements and FDA guidelines for RF power deposition were observed. On both scanners the same stimulated echo method with complete outer volume suppression (Fig. 1) was used to obtain single volume spectra or spectroscopic images at echo times as short as 7 ms. Details of the pulse sequence have been described earlier (18). Slice selective 4-ms sinc pulses were used for the stimulated echo part of the pulse sequence and 6-ms sinc pulses were used for outer volume suppression.

MRM 33:246–252 (1995)

From the Diagnostic Radiology Department, Warren Grant Magnuson Clinical Center (S.P., D.L.B.), Laboratory of Diagnostic Radiology Research (C.A.C.), Section on Clinical Pharmacology, National Institute of Mental Health (R.R.), Laboratory of Cardiac Energetics, National Heart, Lung and Blood Institute (R.S.B.), The National Institutes of Health, Bethesda, Maryland.

Stefan Posse, Ph.D., Institute of Medicine, Research Center Jülich GmbH, P.O. Box 1913, D-52425 Jülich, Germany.

Received May 2, 1994; revised August 15, 1994; accepted October 4, 1994.

0740-3194/95 \$3.00

Copyright © 1995 by Williams & Wilkins

All rights of reproduction in any form reserved.

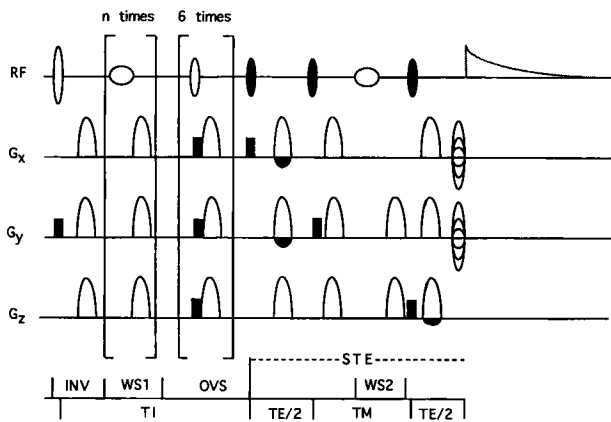


FIG. 1. Water suppressed stimulated echo (STE) pulse sequence with complete outer volume suppression (OVS). The three stimulated echo (STE) pulses are depicted as grey symbols. Slice selection gradient pulses are shown in black. Six outer volume suppression (OVS) pulses are applied to suppress all regions adjacent to the volume of interest. CHES water suppression pulses are applied during WS1 ($n = 3$ at 4 Tesla, $n = 1$ at 1.5 Tesla) and during WS2. A slice selective hyperbolic secant inversion pulse (INV) is added for inversion recovery measurements. Phase encoding gradients for spectroscopic imaging are applied after the third STE pulse.

Water suppression was achieved by single-lobe CHES pulses (sinc profile) with a nominal bandwidth of 200 Hz at 4 Tesla and 75 Hz at 1.5 Tesla, which were placed before the localization scheme ($n = 1$ at 1.5 Tesla and $n = 3$ at 4 Tesla) and during the TM period ($n = 1$). At 4 Tesla, the three CHES pulses before the localization scheme were tuned individually to compensate for the inhomogeneous B_1 -profile of the surface coil (see below). The minimum TM period at 4 Tesla was 33 ms (56 ms at 1.5 Tesla due to longer water suppression pulses). The pulse sequence was designed to exhibit minimum motion sensitivity by placing the TE dephasing gradient pulses closely around the TM period. Localized spectra were acquired from 8 cc volumes in occipital and temporal regions, mostly located in white matter. At 4 Tesla, a 5-inch surface coil for transmission and reception was used. At 1.5 Tesla body-coil transmission and 5-inch surface coil reception was used. Localized shimming was performed manually. On spherical phantoms filled with deionized water and using the same acquisition parameters as *in vivo*, a water line width between 1 and 2 Hz was routinely obtained. This suggests that linebroadening due to eddy current effects was only minor.

T_1 measurements at 4 Tesla on five subjects were obtained with an inversion recovery sequence under fully relaxed conditions. The pulse sequence described above was extended by adding a slice selective 6-ms hyperbolic secant inversion pulse. Due to software limitations with complex pulse sequences the outer volume suppression was limited to a coronal slice posterior to the volume of interest. An echo time of 50 ms was chosen to minimize spectral overlap with multiplet resonances from J -coupled metabolites and from cytosolic proteins. Inversion times (T_I) ranged from 0.15 to 4 s with the repetition time $TR = T_I + 10$ s.

Apparent T_2 -values at $TM = 33$ ms were obtained on five subjects by measuring spectra at nine echo times ranging from 20 to 400 ms. Additional measurements on six subjects were conducted with TM -values of 33, 200, 400, and 800 ms and using only four different echo times (50, 100, 200, 400 ms) at each TM -value to determine the potential influence of diffusion in local tissue related gradients on the apparent T_2 . In some cases the range of measured TM values was limited to three or two TM values (six subjects at $TM = 33$ ms, four subjects at $TM = 200$ ms, two subjects at $TM = 400$ ms, and five subjects at $TM = 800$ ms) due to time constraints and technical problems. At $TM = 800$ ms, the data point obtained at $TE = 400$ ms was discarded in all cases, because the signal-to-noise ratio was too low for quantitation. Diffusional attenuation due to the applied localization gradients was negligible (b_{max} at $TM = 800$ ms was 56 s/mm²). For comparison, further relaxation measurements were conducted on the nonsuppressed water resonance *in vivo* and on cylindrical water phantoms with physiological metabolite solutions of Cho, Cr, and NAA.

Spectra were reconstructed by exponential line-broadening (3 Hz at 4 Tesla and 1 Hz at 1.5 Tesla) Fourier transformation and zero order phase correction. Spectra obtained at different inversion times were quantitated by manually defining a baseline and by measuring peak heights. Spectra obtained at different echo times were quantitated using lorentzian line fitting based on peak positions reported in the literature (19–22). The results were fitted with single exponential functions. In order to assess contributions to the apparent T_2 signal decay *in vivo* from spectral overlap with neighboring multiplet resonances, the spectra from the initial five subjects were reanalyzed by limiting the fit to six spectra with echo times ranging from 50 to 400 ms.

In order to evaluate the possible influence of diffusion in local susceptibility related gradients on the signal decay, normalized NAA signal intensities at different TE s were plotted versus TM . These signal intensities were computed by normalizing signal intensities within each subject to the extrapolated signal intensity at $TE = 0$ ms and $TM = 0$ ms, and by averaging the results over the six subjects. The experimental data were fitted with (23):

$$\ln(S/S_0) = (TE/T_2 + D(\gamma GTE)^2(TM/4 + TE/12) + TM/T_1) \quad [1]$$

where S_0 is the extrapolated signal at $TE = 0$ ms, γ is the gyromagnetic ratio and D is the diffusion coefficient for NAA (0.18×10^{-3} mm²/s) (24). The slope k of the plot $\ln(S/S_0(TE))$ versus TM is given by:

$$k = (D(\gamma GTE)^2)/4 + 1/T_1 \quad [2]$$

Diffusion would result in a quadratic increase with TE of the first term in Eq. [2].

RESULTS

Spectral localization with several hundred-fold water suppression and minimal surface lipid contamination

was obtained at both field strengths (Fig. 2). The line widths in parts per million of major singlet resonances did not significantly differ at both field strengths (between 0.03 and 0.04 ppm in 8 cc volumes depending on the volume localization) despite considerable effort with higher order shimming. Spectral overlap and residual eddy current effects had only minor effects on the measured line width as verified by quantitating spectra at different echo times (20, 50, and 100 ms). This suggests that local susceptibility related gradients within the voxel which cannot be compensated by shimming dominate the line width. By contrast, multiplet resonances were significantly better resolved at 4 Tesla resulting in considerably decreased spectral overlap at short echo times, in particular for NAA.

T_1 -measurements *in vivo* were obtained at five different inversion times (Fig. 3). While most metabolite resonances exhibited similar relaxation behavior, cytosolic proteins and/or residual lipid signals exhibited much faster longitudinal relaxation, as expected. The signal intensities of Cho, Cr, and NAA versus TI closely followed a single exponential function (Fig. 4), as expected. T_1 -values of Cho, Cr, and NAA obtained in occipital brain in five subjects at 4 Tesla (Table 1) were only slightly larger than those reported in the literature at 1.5 Tesla (6). The inversion efficiency of the hyperbolic secant pulse was determined by extrapolating the signal intensity of NAA *in vivo* to TI = 0 ms and to TI = infinity. The magnitude of the two extrapolated signals differed by less than 3%, suggesting that the inversion efficiency of the hyperbolic secant pulse was better than 97% *in vivo*.

Transverse relaxation measurements at 4 Tesla in occipital brain revealed much stronger signal losses in the major singlet resonances with increasing echo time than

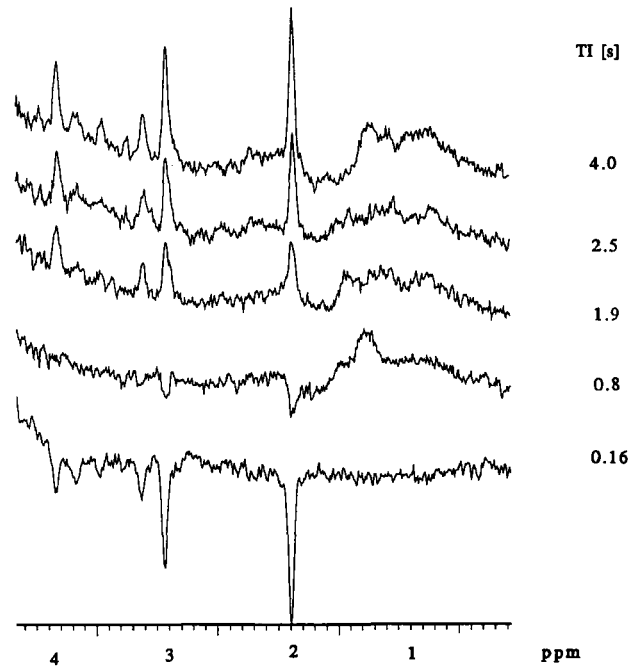


FIG. 3. Spectra from occipital brain obtained at different inversion times ranging from 160 to 4000 ms at 4 Tesla. Residual lipid contaminations and minor contributions from cytosolic proteins between 0 and 2 ppm exhibit shorter T_1 -values and recover faster (TE : 50 ms, TR : TI + 10 s, TM : 34 ms, 8 cc, 64 averages).

at 1.5 Tesla (Figs. 5 and 6). Apparent T_2 -values of Cho, Cr, NAA at 4 Tesla were almost a factor of 2 smaller than those at 1.5 Tesla (Table 2). The degree of apparent T_2 -shortening was also different between these metabolites. Apparent T_2 -values obtained at 1.5 Tesla in one volun-

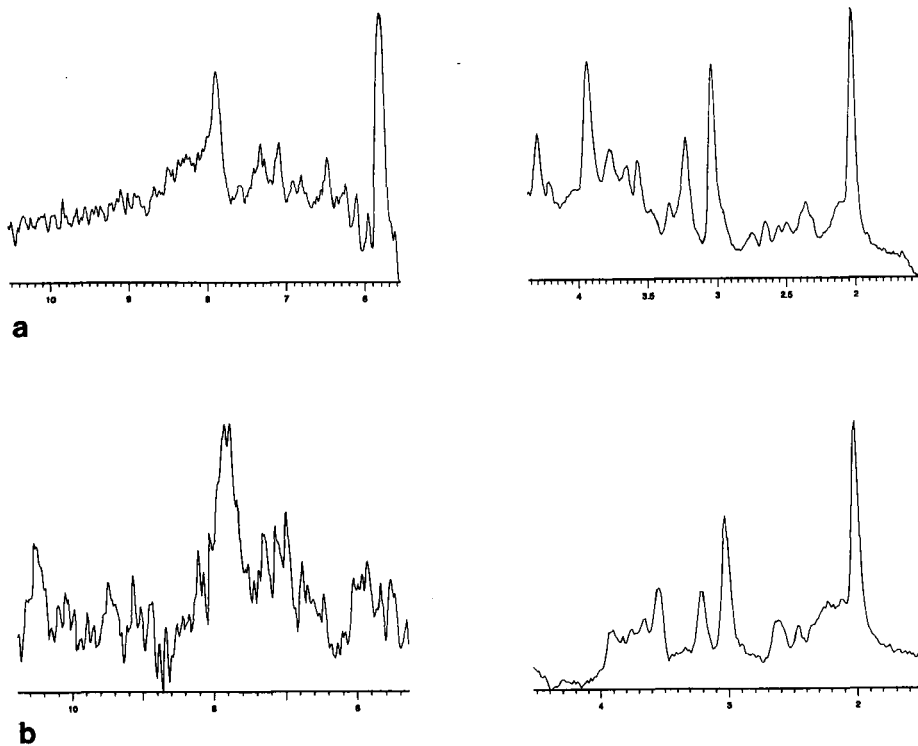


FIG. 2. (a) Typical proton spectrum at short echo times obtained at 4 Tesla in occipital brain using a 5-inch surface transmit/receive coil (TE : 14 ms, TR : 4 s, TM : 33 ms, volume: 8 cc, 256 averages). (b) Typical proton spectrum at short echo times from occipital brain obtained on a clinical 1.5 Tesla whole body scanner using a 5-inch surface receive coil (TE : 14 ms, TR : 4 s, TM : 56 ms, volume: 8 cc, 128 averages). Note the improved resolution of multiplet resonances at 4 Tesla (e.g., glu at 2.35 ppm) and the improved water suppression that allows measuring resonances close to the water line (4.7 ppm). At the left side of water several resonances are visible at 4 Tesla which are difficult to measure at 1.5 Tesla.

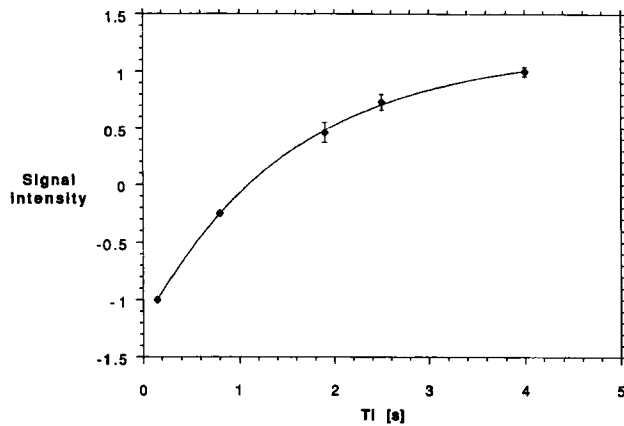


FIG. 4. Normalized signal intensity of NAA in occipital brain versus inversion time at 4 Tesla averaged over five subjects. The solid line represents an exponential fit to the experimental data. Error bars represent the standard deviation.

Table 1

T_1 Values of Metabolites in Human Brain at 4 Tesla

	Cho	Cr	NAA
4 T ($N = 5$)	1.29 (0.17)	1.72 (0.3)	1.63 (0.17)
Ref. 3 (1.5 T)	1.15	1.55	1.45

$S \pm SD$.

Occipital brain, mostly white matter.

teer were consistent with literature values. Apparent T_2 -values in occipital and lateral frontal regions at 4 Tesla were very similar. When limiting the quantitation to spectra with echo times between 50 to 400 ms, to investigate contributions from spectral overlap with neighboring multiplet resonances, the apparent T_2 -values increased by less than 10%. This indicates that at 4 Tesla a satisfactory monoexponential fit can be obtained for the

major singlet resonances, even when including data at short echo times. At 1.5 Tesla this is more difficult due to increased spectral overlap. However, due to sensitivity constraints we did not attempt to further evaluate possible multiexponential signal decay. Motion artifacts due to head movements and cardiac related brain pulsations were insignificant as verified by: (a) storing each acquisition separately prior to Fourier transformation, individual phasing and spectral summation, (b) 2-dimensional spectroscopic imaging of the localized voxel, (c) peripheral gating, and (d) additional head restraints.

Additional measurements on six subjects at different TM-values revealed that the apparent T_2 -values of the metabolites decreased with increasing TM (Fig. 7). The apparent T_2 -value of nonsuppressed water was slightly less sensitive to changes in TM. Within the sensitivity constraints of our measurements the difference in apparent T_2 decrease with TM between NAA and brain water was not statistically significant ($P < 0.05$). The apparent T_2 -values of the metabolites at TM = 33 ms in this experiment were slightly larger with larger error margins than those in the previous experiment, probably due to the smaller number of echo times used. The normalized NAA signal intensities versus TM, plotted at different echo times (Fig. 8), were fitted with Eq. [1] using the measured T_1 -values and apparent T_2 -values at TM = 33 ms. The logarithm of the normalized NAA signal was a linear function of TM, but the slopes k (Eq. [2]) from the fits did not exhibit a quadratic dependence on TE . Thus, further dephasing mechanisms in addition to diffusion in local susceptibility related gradients are likely to contribute to the signal decay with TE and TM.

On phantoms with metabolite solutions a slight increase of the apparent T_2 -values with increasing field strength was measured, as expected (Table 3).

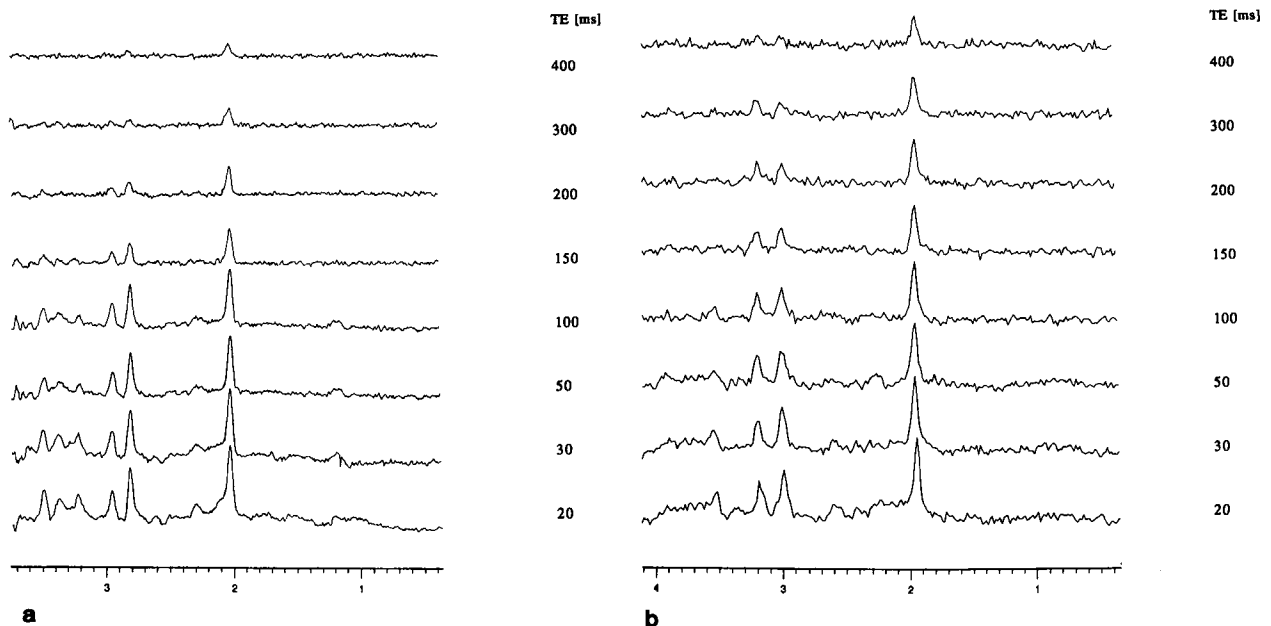


FIG. 5. Spectra from occipital brain obtained at different echo times ranging from 20 to 400 ms at (a) 4 Tesla and (b) 1.5 Tesla. Note the strong signal losses with increasing echo time at 4 Tesla as compared to 1.5 Tesla. (TR : 4 s, TM: 56 ms at 1.5 Tesla and 33 ms at 4 Tesla, 8 cc, 64 averages).

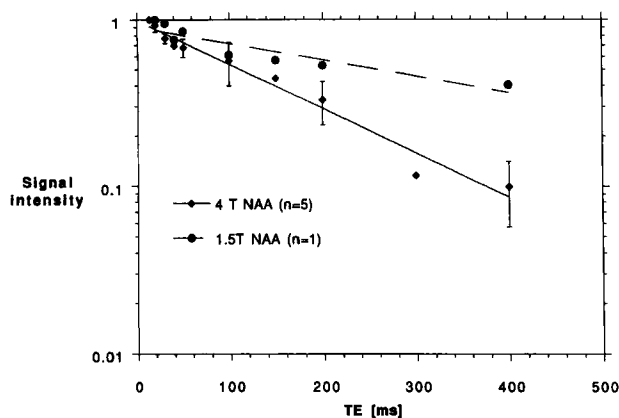


FIG. 6. Normalized NAA signal intensity versus echo time at 1.5 and 4 Tesla in semi-logarithmic display. The solid and dashed lines represent exponential fits to the experimental data. Error bars represent the standard deviations over five subjects measured at 4 Tesla.

Table 2

Apparent T_2 Values of Metabolites in Human Brain Between 1.5 and 4 Tesla

	Ino	Cho	Cr	NAA
4 T (N = 5)	57 (20)	142 (34)	140 (13)	185 (24)
1.5 T (N = 1)	66	305	201	440
Ref. 3 (1.5 T)	110	330	240	450
Ref. 5 (1.5 T)		244	217	400
Ref. 2 (2.1 T)			155	532

ms \pm SD.

Occipital brain, mostly white matter.

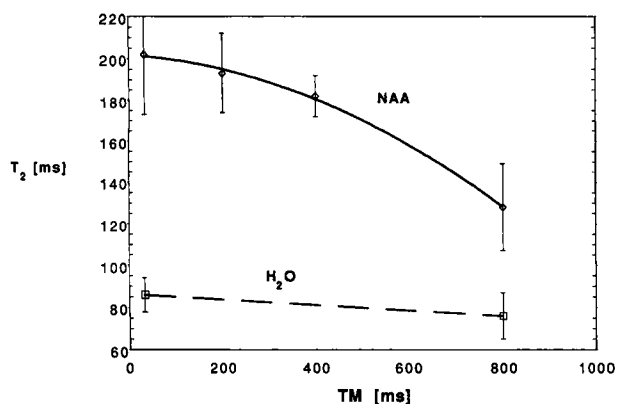


FIG. 7. Apparent T_2 of NAA (averaged over six subjects) and water (averaged over three subjects) versus TM at 4 Tesla in occipital brain. The solid and dashed lines were drawn manually. Error bars indicate the standard deviations which in this experiment are larger for the metabolite resonances due to the smaller number of echo times measured. Smaller error bars for NAA at TM = 400 ms are due to a smaller number of subjects ($n = 2$) measured at that echo time.

DISCUSSION

The T_1 -values are not significantly different at 1.5 and 4 Tesla. These observations are not surprising when compared with the relaxation dispersion of water which exhibits similar spin-lattice relaxation mechanisms. The field dependence of the T_1 -value of brain water decreases

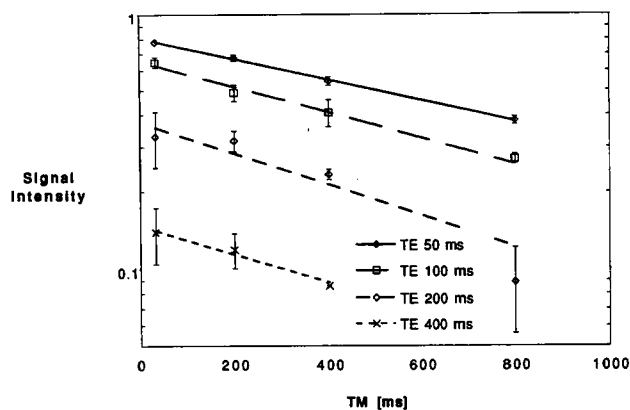


FIG. 8. Normalized signal intensity of NAA versus TM at different TEs, averaged over six subjects. The signal intensity in each experiment was normalized to the signal intensity obtained at TE = 0 ms and TM = 0 ms. The data were fitted with Eq. [1] to determine the possible influence of diffusion on signal losses.

Table 3

Apparent T_2 Values of Metabolites *In Vitro* at 1.5 and 4 Tesla

	Cho	Cr	NAA
4 T	1268 (141)	828 (128)	987 (98)
1.5 T	1048 (58)	595 (57)	827 (28)

ms \pm SD.

toward higher field strengths (25, 26). Our T_1 -values are slightly larger than those reported by Hetherington *et al.* (13), who used an inversion recovery spin echo technique with a repetition time of 2 s. The smaller T_1 -values in their study may be due to the smaller range and fewer number of values used.

The reduction of apparent T_2 -values of the metabolite resonances at 4 Tesla is unexpected. Although the apparent T_2 -value measured with this method reflects a superposition of several dephasing mechanisms, including the true T_2 , it is a key parameter for the signal to noise ratio obtained with long echo time proton spectroscopy *in vivo*. B_1 -inhomogeneities with surface coil transmission are known to introduce signal modulations with increasing echo time in coupled spin systems (27). However, singlet resonances such as Cho, Cr, and NAA are not affected by B_1 -inhomogeneities except for a general decrease in the signal-to-noise ratio due to the nonuniform flip angle distribution over the voxel. Thus, our transverse relaxation measurements of Cho, Cr, and NAA are not influenced by B_1 -inhomogeneities. Spectral overlap (NAA with β -CH₂ of Glu) and changes in coupling patterns at 4 T are confounding factors; however, they are small as we have shown when limiting the number of echo times for quantitation, and we do not believe that they account for the strong signal losses seen at long echo times in all major singlet resonances. Increased motion effects at 4 Tesla, due to gradient vibrations for example, may play a role, but their contributions are probably small, as verified by the different motion compensation methods we have used and by the much larger apparent T_2 -values in our phantom experiments. Diffusion in local susceptibility related gradients may be a contributing factor, but as shown above it is likely that that additional

not yet determined dephasing mechanisms are contributing to the signal loss with *TE* and *TM* as well. Dipolar relaxation by deoxygenated paramagnetic blood and traces of molecular oxygen may be a contributing factor which may mask some of the diffusion effects. Indeed, *in vitro* experiments on superfused guinea pig brain slices at 8.5 T indicate that the apparent T_2 -values of brain metabolites change with oxygenation status (28). However, further experiments with a larger range of *TM* and *TE* values and better sensitivity are needed to investigate these phenomena. Anomalies in the *TM* dependence of the Cho and Cr at 1.5 Tesla which have been reported earlier (6) may be related to our observations at 4 Tesla. Recently, Dreher and coworkers have shown that magnetization transfer reduces the Cr signal intensity at 4.7 Tesla (29). Although exchange phenomena in the Cr signal may be related to the relaxation effects seen in this study, the lack of magnetization transfer effects on Cho and NAA rules out major contributions from exchange phenomena. For water the dependence of the apparent T_2 -values on *TM* at 4 Tesla is slightly less pronounced, probably due to the shorter intrinsic T_2 at 4 Tesla.

Our apparent metabolite T_2 -values are slightly smaller than those reported by Hetherington *et al.* (13), who used a spectroscopic imaging spin echo technique with inversion recovery fat suppression. In white matter they report T_2 -values of 170 ms (\pm 20 ms) for Cho, 144 ms (\pm 19 ms) for Cr, and 234 ms (\pm 26 ms) for NAA. The smaller number of echo times in their study (compare with Fig. 7) may in part be responsible for the difference in apparent T_2 -values.

In conclusion, *TR* will not adversely affect the expected enhancement of signal to noise at 4 Tesla. The decrease in apparent metabolite T_2 -values at 4 Tesla will decrease the predicted signal-to-noise enhancement over lower field strengths, especially at long echo times. This suggests that short echo time spectroscopy is advantageous to maintain signal-to-noise at 4 Tesla. Spectral identification and quantitation at short echo times are facilitated considerably as compared with 1.5 Tesla due to the increased multiplet resolution.

ACKNOWLEDGMENTS

The authors thank Andrew S. Chesnick and GE Medical Systems for hardware and software support, Dr. Fred Heinemann for help with volunteer studies.

REFERENCES

1. S. R. Williams, E. Proctor, K. Allen, D. G. Gadian, H. A. Crookard, Quantitative estimation of lactate in brain by ^1H NMR. *Magn. Reson. Medicine* **7**, 425–431 (1988).
2. C. C. Hanstock, D. L. Rothman, J. W. Pritchard, T. Jue, R. G. Shulman, Spatially localized ^1H NMR spectra of metabolites in the human brain. *Proc. Natl. Acad. Sci. (USA)* **85**, 1821–1825 (1988).
3. J. Frahm, H. Bruhn, M. L. Gyngell, K. D. Merboldt, W. Hänicke, R. Sauter, Localized proton NMR spectroscopy in different regions of the human brain in vivo. Relaxation times and concentrations of cerebral metabolites. *Magn. Reson. Med.* **11**, 47–63 (1989).
4. A. A. De Graaf, W. M. M. J. Bovee, Improved quantification of *in vivo* ^1H NMR spectra by optimization of signal acquisition and processing and by incorporation of prior knowledge into the spectral fitting. *Magn. Reson. Med.* **15**, 305–319 (1990).
5. P. C. M. van Zijl, C. T. W. Moonen, Information content of *in vivo* proton MR spectra of brain, in "Proc. of SMRM, 9th Annual Meeting, 1990," p. 67.
6. P. A. Narayana, D. Johnston, D. P. Flamig, *In vivo* proton magnetic resonance spectroscopy studies of human brain. *Magn. Reson. Imaging* **9**, 303–308 (1991).
7. G. D. Graham, A. M. Blamire, D. L. Rothman, O. A. C. Petroff, J. W. Pritchard, Proton *in vivo* relaxation times of lactate and other metabolites in infarcted human brain tissue, in "Proc., SMRM, 12th Annual Meeting, 1993," p. 1482.
8. D. C. Shungu, J. D. Glickson, Spatially localized relaxometry: mapping of ^1H metabolite T_2 's in the rat brain, in "Proc., SMRM, 12th Annual Meeting, Berkeley, 1993," p. 1510.
9. K. Kamada, K. Houkin, K. Hilda, H. Matsuzawa, Y. Iwasaki, H. Abe, T. Nakada, Localized proton spectroscopy of focal brain pathology in humans: significant effects of edema on spin-spin relaxation time, in "Proc., SMRM, 12th Annual Meeting, 1993," p. 1566.
10. H. Barfuss, H. Fischer, D. Hentschel, R. Ladebeck, J. Vetter, Whole body MR imaging and spectroscopy with a 4 Tesla system. *Radiology* **169**, 811–816 (1988).
11. H. Bomsdorf, T. Helzel, D. Kunz, P. Röschmann, O. Tschendel, J. Wieland, Spectroscopy and imaging with a 4 Tesla whole-body MR system. *NMR Biomed.* **1**(3), 151–158 (1988).
12. H. Barfuss, H. Fischer, D. Hentschel, R. Ladebeck, A. Oppelt, R. Wittig, W. Duerr, R. Oppelt, *In vivo* magnetic resonance imaging and spectroscopy of humans with 4 T whole-body magnet. *NMR Biomed.* **3**(1), 31–45 (1990).
13. H. P. Hetherington, J. W. Pan, G. F. Mason, S. L. Ponder, D. B. Twieg, J. T. Vaughan, G. M. Pohost, High resolution ^1H spectroscopic imaging of human brain at high fields: quantitative evaluation of gray and white matter metabolite differences, in "Proc. SMRM 12th Annual Meeting, 1993," p. 127.
14. S. Posse, C. A. Cuenod, A. S. Chesnick, R. Risinger, R. S. Balaban, D. Le Bihan, Spectral resolution and assignments in short *TE* ^1H spectroscopy in human brain at 4 Tesla, in "Proc., SMRM, 12th Annual Meeting, 1993," p. 128.
15. G. F. Mason, J. W. Pan, H. P. Hetherington, S. Ponder, D. Twieg, G. Pohost, Short echo spectroscopic imaging of glutamate at 4.1 Tesla in human brain *in vivo*, in "Proc., SMRM, 12th Annual Meeting, 1993," p. 368.
16. P. A. Bottomley, T. H. Foster, R. E. Argersinger, L. M. Pfeifer, A review of normal tissue hydrogen NMR relaxation times and relaxation mechanisms from 1–100 MHz: dependence on tissue type, NMR frequency, temperature, species, excitation and age. *Med. Phys.* **11**(4), 425–448 (1985).
17. S. Posse, C. A. Cuenod, R. S. Balaban, D. Le Bihan, Anomalous transverse relaxation in ^1H spectroscopy in human brain at 4 Tesla, in "Proc., SMRM, 12th Annual Meeting 1993," p. 371.
18. S. Posse, B. Schuknecht, M. E. Smith, P. C. M. van Zijl, N. Herschkowitz, C. T. W. Moonen, Short echo-time proton spectroscopic imaging. *J. Comput. Assist. Tomogr.* **17**(1), 1–14 (1993).
19. C. Arus, Y. Chang, M. Barany, Proton nuclear magnetic resonance spectra of excised rat brain. Assignment of resonances. *Physiol. Chem. Phys. Med. NMR* **17**, 23–33 (1985).
20. T. W. M. Fan, R. M. Higaschi, A. N. Lane, O. Jardetzky, Combined use of ^1H -NMR and GC-MS for metabolite monitoring and *in vivo* ^1H -NMR assignments. *Biochim. Biophys. Acta* **882**, 154–167 (1986).
21. O. A. C. Petroff, D. D. Spencer, J. R. Alger, J. W. Pritchard,

- High-field proton magnetic resonance spectroscopy of human cerebrum obtained during surgery for epilepsy. *Neurology* **39**, 1197–1202 (1989).
22. P. C. M. van Zijl, C. T. W. Moonen, In situ changes in purine nucleotide and *N*-acetyl concentrations upon inducing global ischemia in the cat brain. *Magn. Reson. Med.* **29**, 381–385 (1993).
 23. J. E. Tanner, Use of the stimulated echo in NMR diffusion studies. *J. Chem. Phys.*, **62** (3), 2532–2536 (1970).
 24. S. Posse, C. A. Cuenod, D. Le Bihan, Proton diffusion spectroscopy in human brain. *Radiology* **188**, 719–725 (1993).
 25. H. Fischer, P. A. Rinck, Y. van Haverbeke, R. N. Muller, Nuclear relaxation of human brain gray and white matter: analysis of field dependence and implications for MRI. *Magn. Reson. Med.* **16**, 317–334 (1990).
 26. R. G. Bryant, D. A. Mendelson, C. C. Lester, The magnetic field dependence of proton spin relaxation in tissues. *Magn. Reson. Med.* **21**, 117–126 (1991).
 27. W.-I. Jung, O. Lutz, Localized double spin-echo proton spectroscopy of weakly coupled homonuclear spin systems. *J. Magn. Reson.* **96**, 237–251 (1992).
 28. R. Kauppinen, S. R. Williams, Nondestructive detection of glutamate by ^1H nuclear magnetic resonance spectroscopy in cortical brain slices from guinea pig: evidence for changes in detectability during severe anoxic insults. *J. Neurochem.* **57**(4), 1136–1144 (1991).
 29. W. Dreher, D. G. Norris, D. Leibfritz, Magnetization transfer affects the proton creatine/phosphocreatine signal intensity: *in vivo* demonstration in the rat brain. *Magn. Reson. Med.* **31**, 81–84 (1994).